Title

Deposition of ammonium and nitrate in the roots of maize seedlings supplied with different nitrogen salts.

Journal

Journal of experimental botany, 63(5)

ISSN

0022-0957

Authors

Bloom, Arnold J
Randall, Lesley
Taylor, Alison R
et al.

Publication Date

2012-03-01

DOI

10.1093/jxb/err410

Peer reviewed

Journal of Experimental Botany, Vol. 63, No. 5, pp. 1997–2006, 2012
doi:10.1093/jxb/err410 Advance Access publication 2 January, 2012
This paper is available online free of all access charges (see http://jxb.oxfordjournals.org/open_access.html for further details)

Journal of Experimental Botany
www.jxb.oxfordjournals.org

RESEARCH PAPER

Deposition of ammonium and nitrate in the roots of maize seedlings supplied with different nitrogen salts

Arnold J. Bloom[1,*], Lesley Randall[1], Alison R. Taylor[2] and Wendy K. Silk[3]

[1] Department of Plant Sciences, University of California at Davis, Davis, CA 95616, USA
[2] Department of Biology and Marine Biology, University of North Carolina, Wilmington, NC 28403, USA
[3] Department of Land, Air and Water Resources, University of California at Davis, Davis, CA 95616, USA

* To whom correspondence should be addressed. E-mail: ajbloom@ucdavis.edu

Received 1 September 2011; Revised 3 November 2011; Accepted 14 November 2011

Abstract

This study measured total osmolarity and concentrations of NH_4^+, NO_3^-, K^+, soluble carbohydrates, and organic acids in maize seminal roots as a function of distance from the apex, and NH_4^+ and NO_3^- in xylem sap for plants receiving NH_4^+ or NO_3^- as a sole N-source, NH_4^+ plus NO_3^-, or no nitrogen at all. The disparity between net deposition rates and net exogenous influx of NH_4^+ indicated that growing cells imported NH_4^+ from more mature tissue, whereas more mature root tissues assimilated or translocated a portion of the NH_4^+ absorbed. Net root NO_3^- influx under $Ca(NO_3)_2$ nutrition was adequate to account for pools found in the growth zone and provided twice as much as was deposited locally throughout the non-growing tissue. In contrast, net root NO_3^- influx under NH_4NO_3 was less than the local deposition rate in the growth zone, indicating that additional NO_3^- was imported or metabolically produced. The profile of NO_3^- deposition rate in the growth zone, however, was similar for the plants receiving $Ca(NO_3)_2$ or NH_4NO_3. These results suggest that NO_3^- may serve a major role as an osmoticant for supporting root elongation in the basal part of the growth zone and maintaining root function in the young mature tissues.

Key words: ammonium, nitrate, osmolarity, root apex, tissue storage, xylem sap.

Introduction

Most plants obtain the majority of their nitrogen through root absorption of NH_4^+ and NO_3^- ions from the soil solution. Roots are thought to assimilate most of the NH_4^+ near the site of absorption to avoid accumulating the high amounts of free NH_4^+ that would dissipate the transmembrane proton gradients required for respiratory electron transport and for sequestering metabolites in the vacuole (Epstein and Bloom, 2005). In contrast, plants can store high concentrations of NO_3^- in their tissues without toxic effect (Goyal and Huffaker, 1984) and may translocate a large portion of this NO_3^- to the shoots (Andrews, 1986). The chemical form of the nitrogen source, NH_4^+ or NO_3^-, influences a myriad of plant processes including responses to CO_2 enrichment (Bloom *et al.*, 2010), and each source elicits distinct patterns of gene expression (Patterson *et al.*, 2010). Nonetheless, characteristics of the root apex under exposure to physiological levels of NH_4^+ or NO_3^- have received relatively little attention.

A previously published study profiled net fluxes of NH_4^+, NO_3^-, and H^+ along the axis of the seminal root in a maize seedling (Taylor and Bloom, 1998). Local influx was measured by depletion of nitrogen from the bathing solution surrounding the root. When nitrogen was supplied as NH_4NO_3, net influx of NH_4^+ was rather uniform (≈1.4 nmol mm^{-1} h^{-1}) through the root cap and root growth zone, When nitrogen was supplied as $Ca(NO_3)_2$, the pattern of nitrogen influx was significantly different: net NO_3^- influx increased from 1.5 nmol mm^{-1} h^{-1} in the root cap to much higher values, 5.4 and 7.6 nmol mm^{-1} h^{-1} at 3.5 and 11 mm, respectively, from the root apex. The presence of NH_4^+ inhibited net NO_3^- influx. This inhibition together with the observed pattern of H^+ fluxes indicated that the entire maize

root apex absorbed more exogenous NH_4^+ than NO_3^- when both forms were present in the medium.

The approach in this study is to compare endogenous 'deposition rates' of NH_4^+ and NO_3^- with the values for net influx of the exogenously supplied nitrogen forms reported in the earlier study. This leads to an understanding of the source and sink relationships for nitrogen in the growing root. Deposition rates (or cell production rates) are defined to be the net rate at which a nutrient (or cell) is added to or removed from the local tissue element. These rates can be calculated from data on tissue concentration (or cell density) and growth velocity (see methods based on Silk and Erickson, 1979). This kinematic approach has illuminated physiology in a number of studies of plant–environment interactions (e.g., Sharp *et al.*, 1990; Girousse *et al.*, 2005). Here, the spatial profiles of the nitrogen concentrations provide information about metabolic function. Moreover, comparison of net deposition to exogenous influx shows whether the net import or export is occurring at a particular location. Finally, this study extends the approach to show the total uptake of nitrogen into a tissue element during its expansion and displacement.

In the following experiments, maize roots were exposed to a nutrient solution that contained (a) NH_4^+ or NO_3^- as sole N sources, (b) both forms together, or (c) no N source. The concentration of NH_4^+ or NO_3^- in the solutions containing them was 0.1 eq m^{-3} N, a level consistent with those found in soil solutions (Epstein and Bloom, 2005). Net deposition rates of NH_4^+ and NO_3^- were calculated and root contents of NH_4^+ and NO_3^- and other solutes were measured along the root axis from the apex to 60 mm and in the xylem sap to assess the relative contributions of NH_4^+ and NO_3^- both to the N budget and to the osmolarity in the apical 60 mm, including the 10 mm that comprised the elongation zone.

Materials and methods

Growth of maize seedlings

Maize seeds (*Zea mays* cv. Dekalb) were surface sterilized in 1% NaClO, rinsed thoroughly with water, imbibed in aerated 1 mol m^{-3} $CaSO_4$ for 6 h, and germinated in the dark on thick paper towelling at 26 °C. Three-day old seedlings were transferred to 5 dm^3 polyethylene containers filled with an aerated nutrient solution comprised of 1 mol m^{-3} $CaSO_4$, 100 mmol m^{-3} KH_2PO_4, and one of 50 mmol m^{-3} $Ca(NO_3)_2$, 100 mmol m^{-3} $NH_4H_2PO_4$, and 100 mmol m^{-3} NH_4NO_3 as the N-source or a solution lacking nitrogen. The pH was adjusted to pH 6.5 with KOH. The containers were wrapped in aluminium foil to minimize exposure of the roots to light. The seedlings were grown for 18–24 h with the shoots receiving 16 h of 600 µmol m^{-2} s^{-1} photosynthetically active radiation from metal halide high-intensity discharge lamps before harvesting the roots. Harvesting was done at the same time each day (others have found no diurnal variation in metabolite concentrations in the maize root system; Walter *et al.*, 2003).

A previous study, conducted nearly concurrently with the analyses of root NH_4^+ and NO_3^- contents in the current study, monitored net H^+ and inorganic N fluxes when NH_4^+ was supplied as a sole source in the form of $(NH_4)_2SO_4$ to minimize pH buffering (Taylor and Bloom, 1998). The current study was not assessing H^+ fluxes and thus supplied NH_4^+ as a sole N source treatment in the form of $NH_4H_2PO_4$ to provide additional pH buffering. It was assumed that the rates and patterns of root net NH_4^+ flux would be similar in both studies because root NH_4^+ absorption is relatively insensitive to the species of accompanying anion (Lycklama, 1963; Jeong and Lee, 1996; Smart and Bloom, 1988) and because the plants were the same genotype, were about the same age, received similar treatment, and had similar root extension rates (compare Taylor and Bloom, 1998 and Bloom *et al.*, 2006).

Growth analysis included calculation of growth trajectories, growth velocities, and relative elemental growth rates from previously published data on cell length profiles in the root growth zones (Taylor and Bloom, 1998). Silk *et al.* (1989) provides the equations. The growth trajectory follows the time course of the spatial position of a material element, such as a cell wall, during its displacement from the root apex. Thus the growth trajectory enabled the conversion of the spatial patterns of NO_3^- to the developmental time course of NO_3^- content associated with a material (real) element of root tissue (Silk and Erickson, 1979).

Determination of osmolarity and chemical concentrations along the maize root

Individual seedling roots were gently blotted dry before they were rapidly (< 2 s) frozen on a thermoelectric cold-plate mounted under a dissecting microscope. Axial sections of 1-mm length were made with a fine razor at 1-mm increments from 1 to 10 mm and at 20, 40, and 60 mm from the apex along each of 10 roots. Root sections from each location were pooled.

Root sections pooled from 10 roots were weighed to estimate fresh mass and then oven dried at 50 °C and weighed to estimate dry mass. Root sections from another 10 roots were placed directly into the sample chamber of a Wescor 5100 Thermocouple Psychrometer to assess osmolarity. Potassium was extracted from sections from a different 10 roots with a solution of 2% acetic acid and analysed using atomic emission spectrometry (Method 303A, 1985). Soluble carbohydrates were extracted with boiling water and analysed via HPLC with mass selective detection (Johansen *et al.*, 1996). Organic acids were extracted with 80% ethanol solution, evaporated under nitrogen at 50 °C, redissolved in 0.1 M H_2SO_4 plus 0.05% EDTA, and analysed via HPLC with UV detection at 195 and 245 nm (Perez *et al.*, 1997). Lastly, sections from 10 other roots were collected in Eppendorf tubes containing 1.5 ml of 1 mol m^{-3} $CaSO_4$, which was adjusted to pH 3 with H_2SO_4, sonicated for 30 min, and centrifuged. The supernatant was withdrawn and analysed for NH_4^+ and NO_3^- as described below. For each N-treatment, there were three or four replicates of sections pooled from 10 roots each for osmolarity, two replicates for potassium, two for soluble carbohydrates, one for organic acids, and at least three for NH_4^+ and NO_3^-. Root chemical concentrations were expressed per segment water volume based on root radius measurements at each location.

Xylem sap collection

Shoots from 4 d seedlings were cut just above the seed, the cut end was blotted with a lint-free paper tissue to collect most of the fluid exuded from the cut cells, and a small conical plastic reservoir, fabricated by trimming a 200 µl Gilson pipette tip, was placed over the stem to collect xylem sap. A sample containing between 5 and 20 µl of sap was taken from the reservoir, the volume measured, and then the volume brought to 1.5 ml with a solution consisting of 1 mol m^{-3} $CaSO_4$ adjusted to pH 3 with H_2SO_4 before NH_4^+ and NO_3^- analysis. Sap NH_4^+ analyses were conducted only for the treatments receiving NH_4^+ as a N source, namely the NH_4NO_3 and $NH_4H_2PO_4$ treatments. Likewise, sap NO_3^- analyses were conducted only for the treatments receiving NO_3^- as a N source, namely the NH_4NO_3 and $Ca(NO_3)_2$ treatments.

NH_4^+ and NO_3^- analysis

To assess NH_4^+ in the samples, this study modified a fluorimetric method based on the reaction of NH_4^+ with *o*-phthalaldehyde (OPA) (Goyal *et al.*, 1988). An autosampler (Shimadzu Sil 9-A, Japan) injected a 50 mm^3 sample into the flow of a buffer solution consisting of 126 mol m^{-3} K_2HPO_4, 74 mol m^{-3} KH_2PO_4, 5 mol m^{-3} OPA, 0.39 dm^3/m^3 β-mercaptoethanol. The stream circulated for several minutes through a cabinet controlled at 64 °C to optimize the NH_4^+–OPA reaction. The NH_4^+–OPA in each sample was quantified using a fluorescence detector (Shimadzu RF-551, Japan) set at 410 nm excitation and 470 nm emission. The time from sample injection to peak detection was 3.4 minutes with a pump flow rate of 2 cm^3 min^{-1}.

Analysis of NO_3^- was conducted via HPLC (Thayer and Huffaker, 1980). Samples of 50 mm^3 were injected into a stream of 35 mol m^{-3} KH_2PO_4 (adjusted to pH 3.0 with H_3PO_4) before being passed into a 100 mm × 4.6 mm column packed with anion exchange resin (Partisil Sax 10 mol m^{-3}, Whatman Laboratory, USA). The absorbance of column eluent was monitored at 210 nm. The time from sample injection to peak detection was 1.8 min.

Estimation of NH_4^+ and NO_3^- deposition rates and potential uptake

Taylor and Bloom (1998) previously published data on the exogenous influx of NH_4^+ and NO_3^- (i.e., the net flux of NH_4^+ and NO_3^- to or from the bathing medium) for locations along the root axis using equation 17 of Henriksen *et al.* (1992). Here, cell length data from Taylor and Bloom (1998) was used to calculate longitudinal growth velocities v_z, where z is distance from the root apex, and the relative elemental growth rate at location z, $\frac{\partial v_z}{\partial z}$, based on equations 2 and 3 from Silk *et al.* (1989). This study compared the exogenous influx to net deposition rates (Silk and Erickson, 1979). The net deposition rate (D) is given by a continuity equation using data on the longitudinal growth velocity v_z and nitrogen metabolite concentration, [N], where t is time and z is the distance from the root apex:

$$D = \frac{\partial [N]}{\partial t} + [N]\frac{\partial v_z}{\partial z} + v_z\frac{\partial [N]}{\partial z}$$

such that the deposition rate equals the local rate of change + growth dilution + convective rate of change.

It was assumed that the NH_4^+ and NO_3^- profiles change slowly relative to growth displacement times and so the local rates of change could be neglected. The spatial derivatives in N concentration, $\Delta N/\Delta z$, were calculated as the average of a two-point forward difference formula and a two-point backward difference formula with the tabulated data on N per mm vs. mm from the apex. Preliminary calculations showed that forward and backward difference formulas gave similar values to within 10%. Values were converted to concentration basis by dividing by the volume of the 1-mm segment and to a weight basis by dividing by segment fresh weight. 'Assimilation' is used in the conventional sense to refer to amide production causing disappearance of NH_4^+ from the measurable pool. 'Translocation' refers to transport out of the local region via the phloem or xylem. Translocation may be toward the root apex or toward the shoot (acropetal or basipetal).

The total amount of NO_3^- taken up by a 'material element' or real piece of tissue during its growth can be calculated by integrating the uptake over time in a special way, following the tissue element through space. Using the notation proposed by Gandar (1983), the segment length at time t, $L(t)$, of the tissue found initially between $z = 1.4$ and 1.5 mm can be expressed as

$$L(t) = z(1.5, t) - z(1.4, t)$$

where z (1.5, t) represents the current position of the particle found initially at 1.5 mm, and z (1.4, t) represents the current position of the particle found initially at 1.4 mm. As shown in Silk *et al.* (1989), the time for the tissue element $t(Z)$ to reach position z (1.5, t) is calculated from $n(z)$, the number of cells between 1.5 mm and the current position:

$$t(Z) = \frac{n(z) \cdot (\text{mature cell length})}{(\text{root elongation rate})}$$

Growth trajectories were interpolated from the discrete cell number values to small increments of time (0.1 h) using the MATLAB cubic spline interpolation routine. Then the total uptake of NO_3^- into the small tissue element was calculated in EXCEL using the observed influx data:

$$(\text{Total uptake}) = \frac{(\text{previous content}) + \text{influx} \cdot L(t) \cdot \Delta t}{L(t)}$$

The total uptake into a moving tissue element was tabulated as a function of time and location on the root and is displayed as a function of time.

Statistical testing

Values are given as mean ± standard error. Root extension, root biomass, root osmolarity, and nutrient concentrations in the root and xylem sap were analysed using a two-way analysis of variance (SAS GLM procedure version 9.1, SAS Institute, Cary, NC) to determine the main effects and interactions between N treatments and position along the root. Effects of treatment or position were considered significant when $P < 0.05$.

Results

Root growth and anatomy

Roots extended at a rate of 2.31 ± 0.10 mm h^{-1} during the experimental period. There were no significant differences in extension rates among the various N treatments. The average root length of 4-day old seedlings used in the study was 101 ± 30 mm. The zero coordinate for measurements of fluxes or concentration was the apex of the root cap, and this extended from 0 to 0.5 mm. The meristem was located in the apical 0.5–2.0 mm. Relative elemental growth rate analysis showed that root cell elongation was most rapid between 3 and 7 mm from the apex, and growth ceased after 10 mm (Taylor and Bloom, 1998).

Neither fresh nor dry mass of the root segments varied significantly among the N treatments, and so the data for N treatments were pooled (Fig. 1A). Fresh mass per segment was lightest just at the apex at 0.77 ± 0.03 mg mm^{-1} ($n = 4$), was relatively constant over the remainder of the root growth zone at 0.99 ± 0.01 mg mm^{-1} ($n = 36$), and increased at 60 mm from the apex to 1.65 ± 0.05 mg mm^{-1} ($n = 4$). Therefore, accumulation of fresh mass for the growth zone averaged 2.29 mg h^{-1} (= 2.31 mm h^{-1} × 0.99 mg mm^{-1}). This mass growth rate is nearly double the value of 1.3 mg h^{-1} reported by Walter *et al.* (2003) in their related study. The difference may be due to differences in maize genotypes, the addition of Ca^{2+} in the medium to stabilize membrane permeabilities (Epstein and Bloom, 2005), or the 40-fold lower nitrogen concentrations supplied in the current study. As in other studies, dry mass per segment declined through the zone of elongation and gradually increased in the more basal regions of the root (Fig. 1A).

Osmolarity and chemical concentrations along maize roots

The total osmolarity did not differ significantly with N treatment (Fig. 1B). It was highest (≈250 mol m^{-3}) in the zone of rapid elongation and lower in the meristem and in the more basal regions of the root (≈200 mol m^{-3}).

K^+ concentration also did not differ significantly with N treatment (Fig. 2A). The general spatial pattern was consistent with studies in the literature (Silk *et al.*, 1986; Sharp *et al.*, 1990; Walter *et al.*, 2003): K^+ increased significantly from the apex reaching a maximum at 3 mm behind (≈100 mol m^{-3}), sharply declined through the remainder of the zone of elongation, and then remained relatively constant (≈30 mol m^{-3}) in the more basal parts of the root.

Malate profiles were strongly dependent on the N treatment. Malate concentrations were negligible throughout the root in the plants receiving only NO_3^- as N source (Fig. 2B). In plants receiving only NH_4^+, the highest malate concentrations (49–58 mol m^{-3}) were found in the growth zones. In plants supplied with NH_4NO_3, the malate concentrations were approximately half of what was found in the plants receiving only NH_4^+. For N-free roots, the meristem was low in malate, but the rapidly expanding tissue and the base of the growth zone had a substantial concentration (≈23 mol m^{-3}. Thus the presence of NO_3^- in the bathing medium seems to repress malate production, while NH_4^+ stimulates it. For the treatments in which malate was measured at 40 and 60 mm, malate concentration in the mature tissue was found to be half the value in the growth zone (Fig. 2B). In contrast, citrate concentration was relatively low (≈4 mol m^{-3}) throughout the root tip in all N treatments (data not shown).

Sucrose was below the detection limit in all of the samples (data not shown). Glucose and fructose concentrations did not differ significantly among the N treatments (Fig. 3). They rose to a maximum in the zone of elongation (reaching ≈90 mol m^{-3} for glucose, Fig. 3A, and ≈40 mol m^{-3} for fructose, Fig. 3B) and declined in the more basal regions. This is a different pattern from those reported for tissues extracted with 80% ethanol and analysed either

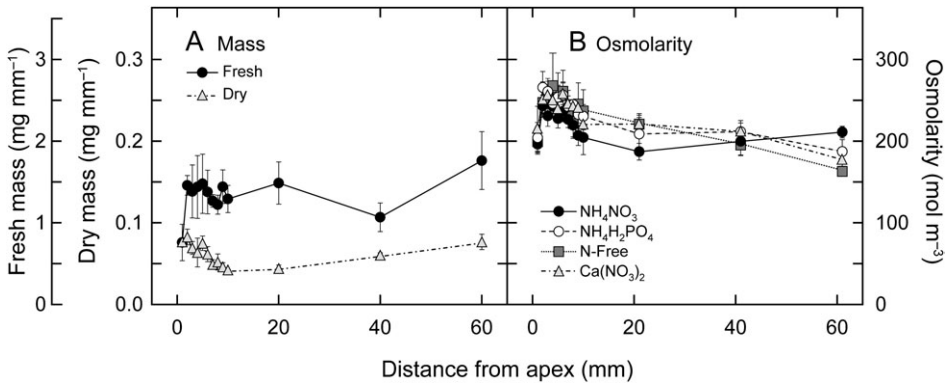

Fig. 1. (A) Fresh and dry mass of 1-mm long radial sections sampled at various distances from the apex of a maize seminal root. Nitrogen source did not influence these parameters significantly and so the data was pooled for the different N sources. Values are means ± SE (10 roots per treatment, three treatments). (B) Osmolarity of radial sections sampled at various distances from the apex of a maize seminal root for plants receiving nutrient solutions that were nitrogen free or contained 100 mmol m^{-3} NH_4NO_3, 100 mmol m^{-3} $NH_4H_2PO_4$, or 50 mmol m^{-3} $Ca(NO_3)_2$. Values are means ± SE ($n = 3$–4).

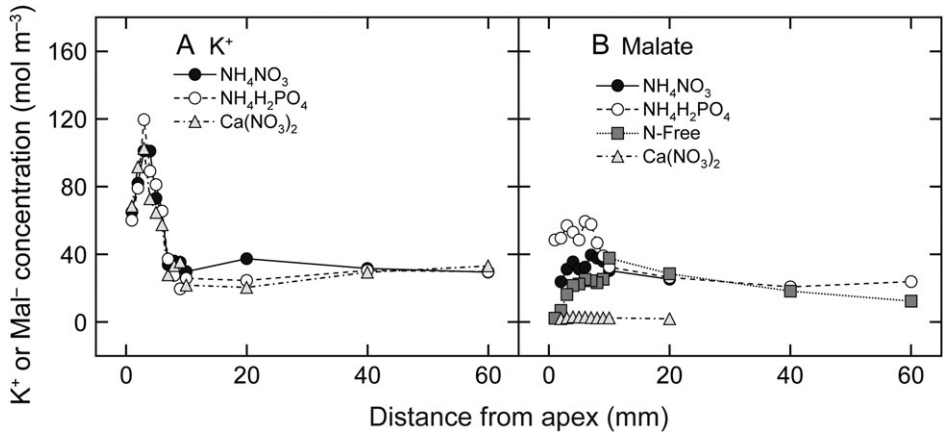

Fig. 2. Tissue concentrations of (A) K^+ and (B) malate at various distances from the apex of a maize seminal root for plants receiving nutrient solutions that contained 100 mmol m^{-3} NH_4NO_3, 100 mmol m^{-3} $NH_4H_2PO_4$, or 50 mmol m^{-3} $Ca(NO_3)_2$ or, for malate, were nitrogen free. Values for K^+ are means ($n = 2$).

colorimetrically (Sharp *et al.*, 1990) or enzymatically (Walter *et al.*, 2003). This study found that 80% ethanol extraction led to variable carbohydrate analyses.

NH_4^+ concentration was fairly uniform along the axis of the seminal root (Fig. 4). Tissue NH_4^+ was significantly higher in the treatments exposed to media containing NH_4^+, but 4 mol m^{-3} tissue NH_4^+ were detected even in the absence of external NH_4^+ (Fig. 4), for reasons that are discussed below.

Tissue NO_3^- was not detectable in the $NH_4H_2PO_4$ treatment (data not shown). Root NO_3^- concentration in the treatments receiving either $Ca(NO_3)_2$ or NH_4NO_3 increased steadily from the apex so that at the base of the growth zone concentrations of NO_3^- exceeded NH_4^+ (Fig. 5). This spatial trend is similar to that Walter *et al.* (2003) reported for roots in complete nutrient medium, even though their nitrogen supply was 40 times greater than that used here and their tissue concentrations were double those found here. Basal to the growth zone, NO_3^- was consistently higher in plants receiving NO_3^- as a sole N-source than in plants receiving both NH_4^+ and NO_3^- (Fig. 5).

The estimate of deposition rate depends on the sum of the spatial derivative in longitudinal growth velocity and the spatial derivative in N concentration. Such derivatives varied widely because growth velocity and N concentration changed dramatically in the zone of elongation (Figs. 1, 4, and 5) and the location of this zone shifted slightly from root to root. Therefore, the variation in the deposition rate was roughly 50% of the mean.

Deposition of NH_4^+ tended to exceed influx of exogenous NH_4^+, but the reverse was true in the more basal regions (Fig. 6A). A similar trend was observed for NO_3^- in the treatment receiving NH_4NO_3, but NO_3^- deposition tended to be slower than exogenous NO_3^- influx along the entire root apex in the treatment receiving $Ca(NO_3)_2$ (Fig. 6B).

Xylem sap NH_4^+ and NO_3^- analysis

The xylem sap contained detectable amounts of NH_4^+ or NO_3^- in the plants receiving the various NH_4^+ or NO_3^- treatments (Fig. 7). NH_4^+ levels in the xylem sap were relatively low (1.4–2.1 mol m^{-3}) and insensitive to the presence of NO_3^- in the nutrient solution (Fig. 7A). In contrast, NO_3^- levels in the xylem sap were nearly an order of magnitude higher than NH_4^+ and doubled when NO_3^- was the sole N source (Fig. 7A).

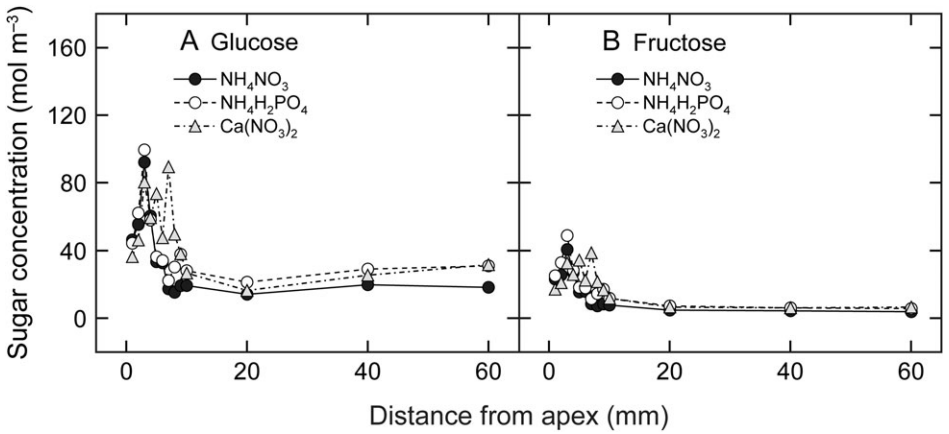

Fig. 3. Tissue concentrations of soluble carbohydrates, (A) glucose and (B) fructose, at various distances from the apex of a maize seminal root for plants receiving nutrient solutions that contained 100 mmol m^{-3} NH_4NO_3, 100 mmol m^{-3} $NH_4H_2PO_4$, or 50 mmol m^{-3} $Ca(NO_3)_2$. Values are means ($n = 2$).

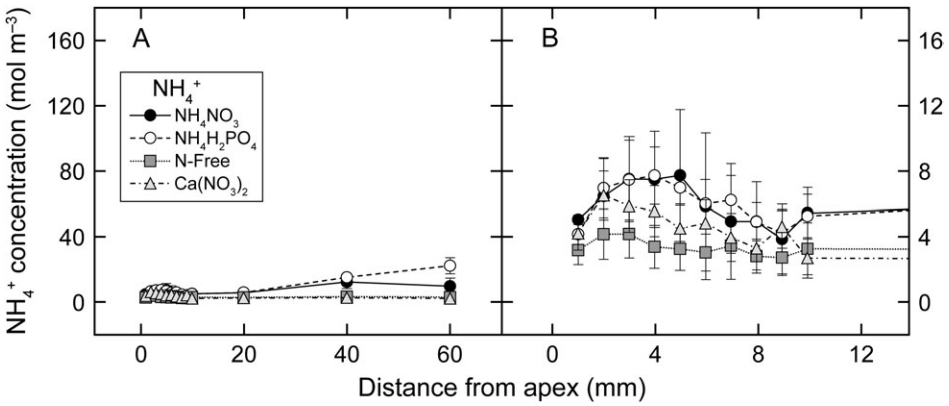

Fig. 4. Tissue concentrations of NH_4^+ at various distances from the apex of a maize seminal root for plants receiving nutrient solutions that were nitrogen free or contained 100 mmol m^{-3} NH_4NO_3, 100 mmol m^{-3} $NH_4H_2PO_4$, or 50 mmol m^{-3} $Ca(NO_3)_2$. (A) All data. (B) Data for locations close to the apex. Values are means ± SE ($n = 3$–6).

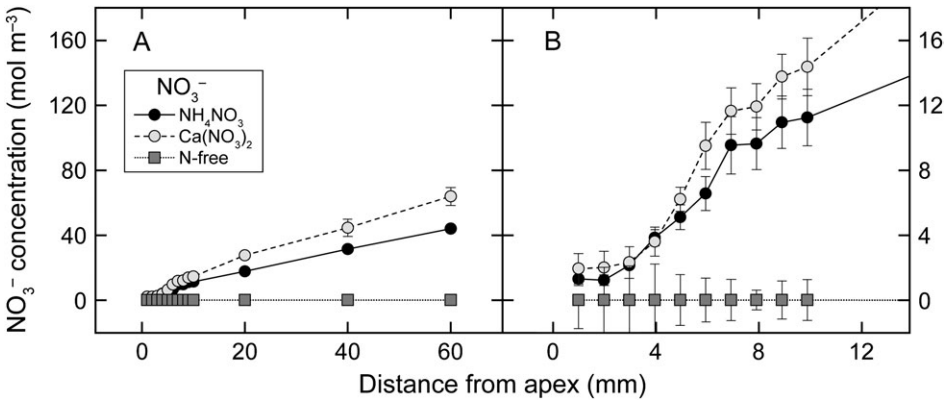

Fig. 5. Tissue concentrations of NO_3^- at various distances from the apex of a maize seminal root for plants receiving nutrient solutions that were nitrogen free or contained either 100 mmol m^{-3} NH_4NO_3 or 50 mmol m^{-3} $Ca(NO_3)_2$. (A) All data. (B) Data for the locations close to the apex. Values are means ± SE (n = 3–6).

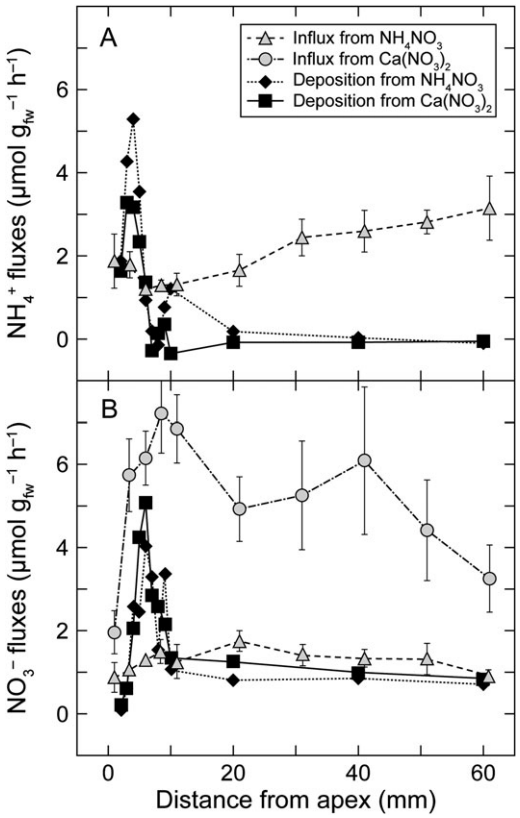

Fig. 6. Influx [based on Taylor and Bloom (1998)] and deposition of (A) NH_4^+ and (B) NO_3^- at various distances from the apex of a maize seminal root for plants receiving nutrient solutions that contained either 100 mmol m^{-3} NH_4NO_3 (n = 6) or 50 mmol m^{-3} $Ca(NO_3)_2$ (n = 9).

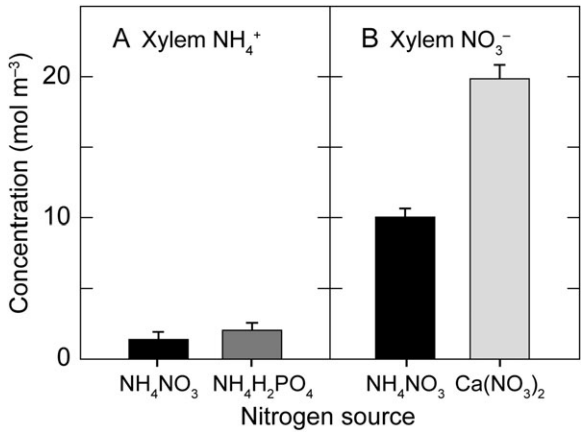

Fig. 7. Concentrations of (A) NH_4^+ and (B) NO_3^- in the xylem sap of maize plants receiving NH_4NO_3, $Ca(NO_3)_2$, or $NH_4H_2PO_4$ as nitrogen sources. Values are mean ± SE (n = 7–13).

Discussion

Fate of N in the root tip supplied with NH_4^+ or NO_3^-: comparison of net influx and deposition rates

The current study is one of the few that has determined both endogenous and exogenous patterns of nutrient supply and the only one that contrasts the two major inorganic N forms, NH_4^+ vs. NO_3^-. A previous report (Taylor and Bloom, 1998) estimated root net influx of exogenous N from the disappearance of N ions from the bathing solution; the current study calculated the endogenous rate at which the N ions are deposited locally with a continuity equation. Comparison of net influx to deposition rate indicates the extent to which the tissue is either retaining or exporting the N taken up from the bathing solution (Fig. 8). If the deposition rate exceeds the exogenous net influx, then the difference shows the rate at which the tissue is importing the ion from older tissue or generating it metabolically.

The fate of absorbed NH_4^+

For roots receiving an exogenous NH_4NO_3, net NH_4^+ influx was fast enough to support the local deposition only in tissue basal to 5 mm (Fig. 6A). Because NH_4^+ deposition rate exceeded the exogenous net influx through the apical 5 mm, the meristem and apical half of the growth zone must retain most of the exogenous supply as well as import NH_4^+ or NH_4^+ precursors from more mature tissue. This conclusion is supported by the observation that similar NH_4^+ deposition rates occurred in the apical 6 mm when the source was $Ca(NO_3)_2$ (Fig. 6A); some combination of chemical

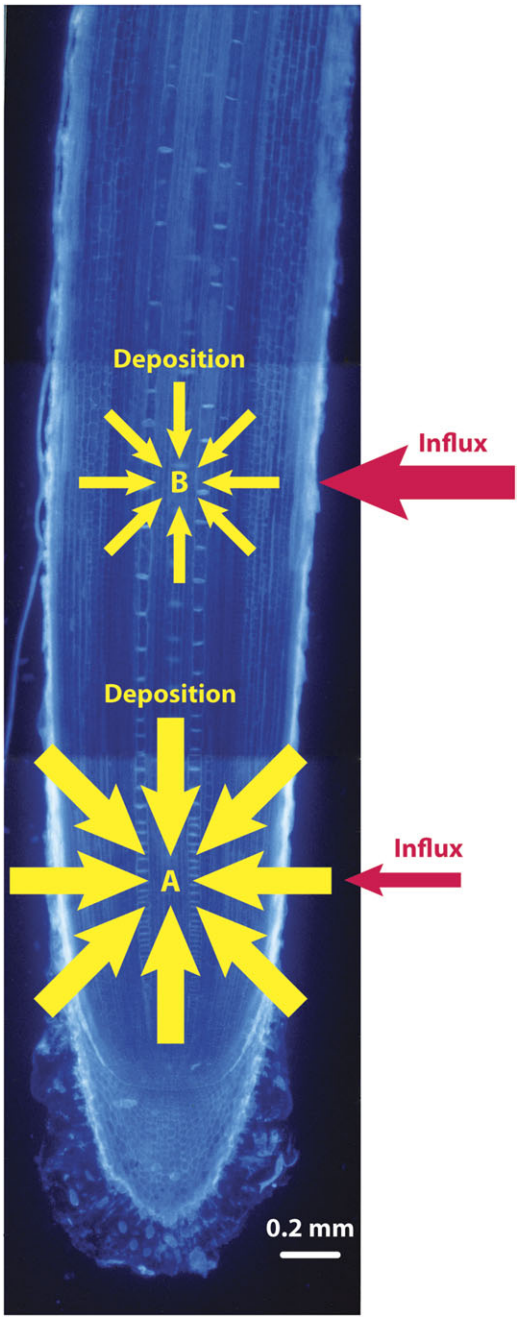

Fig. 8. The maize root apex. At location A, deposition of a substance (e.g., NH_4^+ or NO_3^-) exceeds influx and so the tissue is importing the substance. At location B, influx exceeds deposition and so the tissue is exporting the substance.

transformation of NO_3^-, import of NH_4^+ from more mature tissue, or deamination of amino acids must have occurred at these locations. With the exogenous $Ca(NO_3)_2$ supply, the NH_4^+ deposition rate becomes small or even negative in the region basal to 6 mm. These conclusions confirm and, by showing the spatial profiles, extend the conclusions of Walter *et al.* (2003), who found that as a whole, the growth zone receives from non-growing tissue 31 nmol h^{-1} NH_4^+ while it exports 45 nmol h^{-1} NO_3^-.

The excess of net influx over deposition of NH_4^+ and the co-occurring decline in tissue NH_4^+ in regions basal to 7 mm (Fig. 4B) suggest that NH_4^+ absorbed near the apex remained unassimilated, whereas NH_4^+ absorbed in the region 7–60 mm from the apex was assimilated (Fig. 4A). Profiles of net NH_4^+ and H^+ fluxes in the maize seminal root also support this interpretation (Colmer and Bloom, 1998; Taylor and Bloom, 1998; Bloom *et al.*, 2002). Assimilation of NH_4^+ produces H^+ that roots rapidly excrete (Allen, 1988). The current study found that net NH_4^+ influx was greater at the root apex than at the regions 4–10 mm from the apex, but that net H^+ efflux was greater 4–10 mm from the apex than at the apex, suggesting that NH_4^+ assimilation was more rapid in the more basal regions (Taylor and Bloom, 1998).

This seems reasonable given the carbon/nitrogen balance in the root apex. The assimilation of NH_4^+ into glutamine is highly carbohydrate dependent, requiring carbon skeletons from 2-oxoglutarate and a respiratory expenditure of about 2 ATP equivalents per NH_4^+ (Bloom *et al.*, 1992). The root apex, however, lacks mature vascular tissue to facilitate carbohydrate translocation from more basal tissues, and nonvascular, symplastic diffusion of carbohydrates appears to be inadequate to meet the energy requirements of this tissue (Bret-Harte and Silk, 1994). Thus, the apex probably suffers from carbohydrate limitations. Maize seminal roots most likely store some of the NH_4^+ absorbed at the apex in vacuoles to avoid toxicity. Indeed, the location of maximum deposition of NH_4^+ (3–6 mm from the apex) coincides with the location where vacuoles in root cells are enlarging. Assimilation of NH_4^+ is greater in more basal regions where the phloem is more fully developed and capable of supplying sufficient carbohydrates.

Although the NH_4^+ concentrations in the N-free and $Ca(NO_3)_2$ treatments were significantly lower than those in the NH_4NO_3 and $NH_4H_2PO_4$ treatments, the N-free and $Ca(NO_3)_2$ treatments still showed small amounts of NH_4^+ in their root growth zones. Several explanations come to mind. First, the extraction and analysis protocols may have resulted in some deamination of amino acids. Second, some of the signal may have come from free amino acids in the root sample because free amino acids interfere with the NH_4^+ analysis technique, although the sensitivity of this analysis to amino acids is less than 10% of its sensitivity to free NH_4^+ (Goyal *et al.*, 1988). It is concluded that the apical 4 mm imported or produced free NH_4^+ through deamination during N-cycling even when NH_4^+ was not present in the bathing solution. When NH_4^+ was present exogenously, the presence of NO_3^- in the medium had only a small effect upon NH_4^+ concentrations in the root tissue (Fig. 4A) or in the xylem sap (Fig. 7A). This fits with earlier studies that demonstrated root NH_4^+ acquisition to be relatively independent of NO_3^- or other anions (Bloom, 1997).

The fate of absorbed NO_3^-

The profile of NO_3^- concentration in the growth zone was the same with $Ca(NO_3)_2$ as with NH_4NO_3 (Fig. 5), but the way in which the patterns were produced varied with the form of nitrogen supplied. With the $Ca(NO_3)_2$ treatment,

NO_3^- influx exceeded the net deposition rate at all locations, but especially in the parts of the root basal to the growth zone where the influx was 4- to 5-fold greater than the deposition rate. The patterns with the NH_4NO_3 treatment were quite different: in the meristem and beyond 12 mm NO_3^- influx slightly exceeded the deposition rate, but throughout the rapid growth zone the deposition rate exceeded influx. Thus, with the $Ca(NO_3)_2$ treatment, the entire root tip absorbed more NO_3^- than it deposited; indeed, the NO_3^- influx greatly exceeded the amount that remained in the tissue. In contrast, with NH_4NO_3 treatment, most of the growth zone was importing NO_3^- from mature tissue and NO_3^- influx greatly exceeded that which remained in the tissues only in the more basal regions (Fig. 5). Thus when NH_4^+ was present in the medium, NO_3^- absorbed near the root apex was stored in the tissue and negligible amounts were assimilated or translocated. It is concluded that the more mature tissues (regions more than 20 mm from the apex) were assimilating and exporting much of the NO_3^- absorbed. This is a reasonable conclusion because NO_3^- influx exceeded the deposition rate in these tissues (Fig. 6B) and NO_3^- in the xylem sap doubled (Fig. 7B).

Lagrangian (tissue-specific) view of NO_3^- uptake

During its development, an individual tissue element is displaced from the root meristem through and then beyond the growth zone. The position of the basal and apical ends of the segment can be tracked to find the location and length of the segment over time. The growth trajectory gives the time course of the element position (distance from the root apex) and can be calculated by integrating the displacement velocity over time (Silk and Erickson, 1979) or (if growth and cell division are steady) by counting the number of cells to the position of interest and multiplying by the ratio of mature cell length to root elongation rate (Silk *et al.*, 1989). This paper is interested in calculating the total uptake of NO_3^- into the tissue element as it expands and moves farther from the apex. To model the 'potential uptake' of NO_3^- that results from influx, this study assumes no assimilation or translocation and then considers what the NO_3^- content would be in the moving tissue element. Before calculating the total uptake in the developing tissue element, two extreme cases are considered: (1) localized influx only in the apical 3 mm; and (2) uniform influx along the growth zone. In the first case, with influx occurring only near the apex (dotted line in Fig. 9A), then the NO_3^- content would first increase (where uptake is faster than growth-associated dilution) and then decrease (at 2–3 mm where growth is faster than influx). Where growth continues after influx ceases, then NO_3^- would decrease more rapidly with position. Where influx and growth have both stopped, NO_3^- would remain uniform (constant with position) in the absence of assimilation and translocation. Therefore, if influx is restricted to the apical 3 mm, the potential uptake into the older root segment would be quite small. In the second case, with influx occurring throughout the root, then the potential uptake would increase slowly as the element moves through the growth zone and more rapidly after growth has ceased in the tissue element (dashed line in Fig. 9A). NO_3^- is in fact taken up throughout the root (Taylor and Bloom, 1998). Fig. 9B shows that the total NO_3^- uptake slightly exceeds the observed content while the tissue element is moving through in the growth zone, and the total uptake vastly exceeds the content when the tissue element is in the 10–20 mm region.

Comparisons of the influx and deposition rates (Figs. 6 and 8) are most useful to analyse the physiology and biochemistry of the local nitrogen transformations and to determine the source–sink relations. It is also instructive, however, to compare the total uptake to the content (Fig. 9B), to appreciate the amount of the influx that has been retained in the tissue element over time.

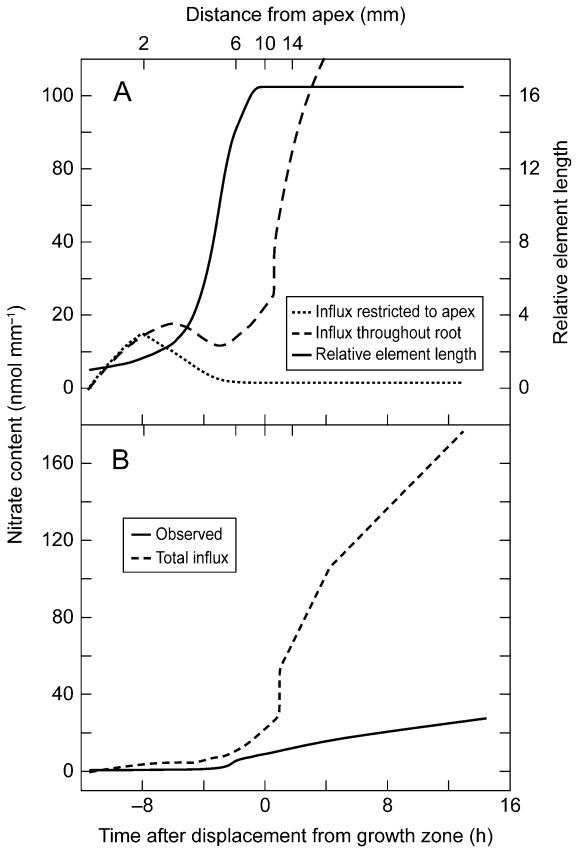

Fig. 9. Models of NO_3^- content (nmol mm^{-1}) and relative element length as a function of the time (bottom axis) or distance (top axis) that a root tissue element is displaced from the base of the growth zone. (A) Model results of potential NO_3^- uptake assuming influx with no translocation or assimilation. This is a material specification in which a material (real) tissue element is followed through time and space. The case of influx restricted to the apical 3 mm is given by the dotted line, and the case of influx throughout the root is shown by the dashed line. The solid line shows the length of the tissue element during the time of its displacement through and beyond the growth zone. (B) Material specification in which the potential uptake and observed content of NO_3^- in a material (real) tissue element is followed through time and space.

Osmolarity

Glucose and fructose contributed about half of the osmolarity in the zone of elongation (Figs. 1B and 3). Sucrose was undetectable (data not shown). Other studies estimated sucrose in the maize root apex from tissues extracted with 80% ethanol at 80 °C and estimated sucrose after its chemical or biochemical conversion to glucose (Sharp *et al.*, 1990; Walter *et al.*, 2003; Ogawa *et al.*, 2005), procedures that can overestimate sucrose and underestimate glucose and fructose (Johansen *et al.*, 1996). The current study directly measured glucose, fructose, and sucrose via HPLC immediately after boiling water extraction to inactivate any enzymes that might hydrolyse sucrose.

K^+ and its counter-ions contributed the other half of the osmolarity in the zone of elongation (Fig. 2A). Previous studies on maize seminal roots have not addressed the issue of counter-ions for K^+ (Silk *et al.*, 1986; Sharp *et al.*, 1990; Rodriguez *et al.*, 1997; Walter *et al.*, 2003). This study found that the counter-ions for K^+ included malate (Fig. 2B) and NO_3^- (Fig. 5), but these could balance less than half of the K^+. The nutrient solution also contained $H_2PO_4^-$ and SO_4^{2-}. Walter *et al.* (2003) measured $H_2PO_4^-$ and SO_4^{2-} along the apical 10 mm of maize seminal roots receiving NH_4NO_3 and found their concentrations to be less than a third of the NO_3^- concentrations. Most likely a combination of these anions, organic anions other than malate and citrate, and an increase in cellular pH accounted for the remainder of the counter-ions (Haynes, 1990).

Osmolarity remained high in the more basal zones of the root (20–60 mm from the apex) despite a substantial decline in glucose, fructose, and K^+ concentrations (Figs. 1B, 2A, and 3). NO_3^- accumulated in these more basal regions, as discussed above, but NO_3^- and its counter-ions such as K^+ contributed less than half of the observed osmolarity (Fig. 5A). Unfortunately, previous studies have not analysed solute concentrations in these more basal regions (Silk *et al.*, 1986; Sharp *et al.*, 1990; Rodriguez *et al.*, 1997; Walter *et al.*, 2003) or have analysed only the soluble sugars (Ogawa *et al.*, 2005). A complete inventory of solutes in maize seminal roots awaits future study.

NH_4^+ vs. NO_3^-

These results indicate that when both NH_4^+ and NO_3^- were available in the rhizosphere, maize roots absorbed both forms, but preferentially assimilated NH_4^+ and stored NO_3^-. Assimilation of NO_3^- to glutamine expends 12 ATP equivalents versus only 2 ATP equivalents for NH_4^+ to glutamine (Bloom *et al.*, 1992). For the root apex, which may be carbohydrate-limited, a 6-fold difference in energy requirements was obviously critical. When NO_3^- was the sole N-source, the root stored about the same amount of NO_3^- in its tissues, while apparently importing or assimilating some NO_3^- to support the rapid protein synthesis in the meristem and translocating a large portion of the NO_3^- from the young mature tissues to the shoot. Shoots can use surplus light to assimilate NO_3^- so that the large energy demands of this process do not detract from growth (Bloom *et al.*, 1989).

The storage of substantial quantities of NO_3^- at the base of the growth zone and in the young mature root tissues argues that NO_3^- may serve as a metabolically benign osmoticant to balance other ions in plant tissues (Hanson and Hitz, 1983; Veen and Kleinendorst, 1986; McIntyre, 1997; Burns *et al.*, 2010). Zhen *et al.* (1991), using intracellular NO_3^--selective microelectrodes, found that most of the NO_3^- in the epidermal and cortical cells of barley roots was stored in the vacuole and at levels that varied between 50 and 100 mol m^{-3}. Here, accumulation of hexoses and K^+ in root cells of the elongation zone sustained root expansion, and malate served as counter-ions to K^+, as it does in other tissues (Osmond, 1976; Niedziela *et al.*, 1993). Synthesis of malate, however, may unduly tax a carbohydrate-limited root apex. Indeed, $Ca(NO_3)_2$ treatment, which accumulated more NO_3^- than the other treatments (Fig. 5), contained negligible amounts of malate (Fig. 2B).

In conclusion, NH_4^+ and NO_3^- differentially affect the fine-scale spatial patterns of uptake, export, assimilation, and carbohydrate content along root apices. Moreover, although NO_3^- levels are maintained low in the meristem and the apical part of the growth zone, NO_3^- clearly needs to be considered as a significant component of the osmotic pool supporting expansion at the base of the growth zone and sustaining the functions of young, mature root tissues.

Acknowledgements

The authors thank Eugene Kim for his technical assistance. This work was funded in part by the National Science Foundation (IOS-08-18435) and the US Department of Agriculture (2008-01029) (to AJB) and the Kearney Foundation of Soil Science (2008.016) (to WKS).

References

Allen S. 1988. Intracellular pH regulation in plants. *ISI Atlas of Science: Animal and Plant Sciences* **1,** 283–288.

Andrews M. 1986. The partitioning of nitrate assimilation between root and shoot of higher plants. *Plant, Cell and Environment* **9,** 511–519.

Bloom AJ. 1997. Interactions between inorganic nitrogen nutrition and root development. *Zeitshrift für Pflanzennährung und Bodenkunde* **160,** 253–259.

Bloom AJ, Burger M, Asensio JSR, Cousins AB. 2010. Carbon dioxide enrichment inhibits nitrate assimilation in wheat and *Arabidopsis*. *Science* **328,** 899–903.

Bloom AJ, Caldwell RM, Finazzo J, Warner RL, Weissbart J. 1989. Oxygen and carbon dioxide fluxes from barley shoots depend on nitrate assimilation. *Plant Physiology* **91,** 352–356.

Bloom AJ, Frensch J, Taylor AR. 2006. Influence of inorganic nitrogen and pH on the elongation of maize seminal roots. *Annals of Botany* **97,** 867–873.

Bloom AJ, Meyerhoff PA, Taylor AR, Rost TL. 2002. Root development and absorption of ammonium and nitrate from the rhizosphere. *Journal of Plant Growth Regulation* **21,** 416–431.

Bloom AJ, Sukrapanna SS, Warner RL. 1992. Root respiration associated with ammonium and nitrate absorption and assimilation by barley. *Plant Physiology* **99,** 1294–1301.

Bret-Harte MS, Silk WK. 1994. Nonvascular, symplasmic diffusion of sucrose cannot satisfy the carbon demands of growth in the primary root tip of *Zea mays* L. *Plant Physiology* **105,** 19–33.

Burns IG, Zhang KF, Turner MK, Edmondson R. 2010. Iso-osmotic regulation of nitrate accumulation in lettuce. *Journal of Plant Nutrition* **34,** 283–313.

Colmer TD, Bloom AJ. 1998. A comparison of NH_4^+ and NO_3^- net fluxes along roots of rice and maize. *Plant, Cell and Environment* **21,** 240–246.

Epstein E, Bloom AJ. 2005. *Mineral Nutrition of Plants: Principles and Perspectives*. Sunderland, MA: Sinauer Associates.

Gandar PW. 1983. Growth in root apices. 1. The kinematic description of growth. *Botanical Gazette* **144,** 1–10.

Girousse C, Moulia B, Silk W, Bonnemain JL. 2005. Aphid infestation causes different changes in carbon and nitrogen allocation in alfalfa stems as well as different inhibitions of longitudinal and radial expansion. *Plant Physiology* **137,** 1474–1484.

Goyal SS, Huffaker RC. 1984. Nitrogen toxicity in plants. In: Hauck RD, ed, *Nitrogen in Crop Production*. Madison, WI: ASA, CSSA, SSSA, pp 97–118.

Goyal SS, Rains DW, Huffaker RC. 1988. Determination of ammonium ion by fluorometry or spectrophotometry after on-line derivatization with *o*-phthalaldehyde. *Analytical Chemistry* **60,** 175–179.

Hanson AD, Hitz WD. 1983. Water deficits and the nitrogen economy. In: Taylor HM, Jordan WR, Sinclair TR, eds, *Limitations to Efficient Water Use in Crop Production*. Madison, WI: ASA, pp 331–343.

Haynes RJ. 1990. Active ion uptake and maintenance of cation-anion balance: a critical examination of their role in regulating rhizosphere pH. *Plant and Soil* **126,** 247–264.

Henriksen GH, Raman DR, Walker LP, Spanswick RM. 1992. Measurement of net fluxes of ammonium and nitrate at the surface of barley roots using ion-selective microelectrodes. II. Patterns of uptake along the root axis and evaluation of the microelectrode flux estimation technique. *Plant Physiology* **99,** 734–747.

Jeong BR, Lee CW. 1996. Influence of ammonium, nitrate, and chloride on solution pH and ion uptake by Ageratum and Salvia in hydroponic culture. *Journal of Plant Nutrition* **19,** 1343–1360.

Johansen HN, Glitso V, Knudsen KEB. 1996. Influence of extraction solvent and temperature on the quantitative determination of oligosaccharides from plant materials by high-performance liquid chromatography. *Journal of Agricultural and Food Chemistry* **44,** 1470–1474.

Lycklama JC. 1963. The absorption of ammonium and nitrate by perennial rye-grass. *Acta Botanica Neerlandica* **12,** 361–423.

McIntyre GI. 1997. The role of nitrate in the osmotic and nutritional control of plant development. *Australian Journal of Plant Physiology* **24,** 103–118.

Method 303A. 1985. Antimony, bismuth, cadmium, calcium, cesium, chromium, cobalt, copper, gold, iridium, iron, lead, lithium, magnesium, manganese, nickel, palladium, platinum, potassium, rhodium, ruthenium, silver, sodium, strontium, thallium, tin and zinc by direct aspiration into an air-acetylene flame. In Greenberg AE, Trussell RR, Clesceri LS, Franson MAH, *eds, Standard Methods for the Examination of Water and Wastewater*. Washington, DC: American Public Health Association, 157–160.

Niedziela CE, Nelson PV, Peet MM, Jackson WA. 1993. Diurnal malate and citrate fluctuations as related to nitrate and potassium concentrations in tomato leaves. *Journal of Plant Nutrition* **16,** 165–175.

Ogawa A, Kawashima C, Yamauchi A. 2005. Sugar accumulation along the seminal root axis, as affected by osmotic stress in maize: a possible physiological basis for plastic lateral root development. *Plant Production Science* **8,** 173–180.

Osmond CB. 1976. Ion absorption and carbon metabolism in cells of higher plants. In: Luttge U, Pitman MG, eds, *Encyclopedia of Plant Physiology, new series*. Berlin: Springer-Verlag, pp 347–372.

Patterson K, Cakmak T, Cooper A, Lager I, Rasmusson AG, Escobar MA. 2010. Distinct signalling pathways and transcriptome response signatures differentiate ammonium- and nitrate-supplied plants. *Plant Cell and Environment* **33,** 1486–1501.

Perez AG, Olias R, Espada J, Olias JM, Sanz C. 1997. Rapid determination of sugars, nonvolatile acids, and ascorbic acid in strawberry and other fruits. *Journal of Agricultural and Food Chemistry* **45,** 3545–3549.

Rodriguez HG, Roberts J, Jordan WR, Drew MC. 1997. Growth, water relations, and accumulation of organic and inorganic solutes in roots of maize seedlings during salt stress. *Plant Physiology* **113,** 881–893.

Sharp RE, Hsiao TC, Silk WK. 1990. Growth of the maize primary root at low water potentials. 2. Role of growth and deposition of hexose and potassium in osmotic adjustment. *Plant Physiology* **93,** 1337–1346.

Silk WK, Erickson RO. 1979. Kinematics of plant growth. *Journal of Theoretical Biology* **76,** 481–501.

Silk WK, Hsiao Theodore C, Diedenhofen U, Matson C. 1986. Spatial distribution of potassium, solutes and their deposition rates in the growth zone of the primary corn root. *Plant Physiology* **82,** 853–858.

Silk WK, Lord EM, Eckard KJ. 1989. Growth patterns inferred from anatomical records – empirical tests using longisections of roots of *Zea mays* L. *Plant Physiology* **90,** 708–713.

Smart DR, Bloom AJ. 1988. Kinetics of ammonium and nitrate uptake among wild and cultivated tomatoes. *Oecologia* **76,** 336–340.

Taylor AR, Bloom AJ. 1998. Ammonium, nitrate, and proton fluxes along the maize root. *Plant, Cell and Environment* **21,** 1255–1263.

Thayer JR, Huffaker RC. 1980. Determination of nitrate and nitrite by high-pressure liquid chromatography: comparison with other methods for nitrate determination. *Analytical Biochemistry* **102,** 110–119.

Veen BW, Kleinendorst A. 1986. The role of nitrate in osmoregulation of Italian ryegrass. *Plant and Soil* **91,** 433–436.

Walter A, Feil R, Schurr U. 2003. Expansion dynamics, metabolite composition and substance transfer of the primary root growth zone of *Zea mays* L. grown in different external nutrient availabilities. *Plant, Cell and Environment* **26,** 1451–1466.

Zhen RG, Koyro HW, Leigh RA, Tomos AD, Miller AJ. 1991. Compartmental nitrate concentrations in barley root cells measured with nitrate-selective microelectrodes and by single-cell sap sampling. *Planta* **185,** 356–361.